

# K-shell ionization cross sections of Cu, Zn and Ge by 3-5 MeV/U Si-ion bombardment

Shashank Singh<sup>1</sup>, Mumtaz Oswal<sup>2</sup>, Sunil Kumar<sup>3</sup>, K.P. Singh<sup>1</sup>, D. Mitra<sup>4</sup> and T. Nandi<sup>5\*</sup>

<sup>1</sup>*Department of Physics, Panjab University, Chandigarh-160014, India.*

<sup>2</sup>*Department of Physics, Dev Samaj College for Women, Sector 45 B, Chandigarh-160014, India.*

<sup>3</sup>*Govt. Degree college, Banjar, Kullu, Himachal Pradesh-175123, India.*

<sup>4</sup>*Department of Physics, University of Kalyani, Kalyani, Nadia-741235, West Bengal, India. and*

<sup>5</sup>*Inter-University Accelerator Centre, Aruna Asaf Ali Marg, Near Vasant Kunj, New Delhi-110067, India.\**

The K x-ray spectra of different targets (Cu, Zn, and Ge) induced by 3 to 5 MeV/u Si projectile ions have been measured to determine the K-shell ionization cross-section. A significant difference is observed between the measurements and theoretical estimates, where the theoretical ones are about 28-35% of the experimental results. Such difference is reduced to a good extent 51-56% if multiple ionization effects are taken into account. Remaining discrepancy may be attributed to the electron capture contribution.

## I. INTRODUCTION

Ionization dynamics of target atoms by energetic heavy ions is important in several fields of research such as material analysis, material engineering, atomic and nuclear physics, accelerator physics, biophysics, medical science, etc. The precise data of ionization cross-section of target atoms are required in case of heavy-ion application in particle-induced x-ray emission (PIXE) [1] and in heavy-ion tumor therapy [2]. Appropriate knowledge of K-shell ionization is essential to determine the elemental concentration during PIXE analysis and to estimate the direct damage of the tumor by the projectiles. Besides the target ionization, the effect of secondary electrons during heavy-ion impact in the patient's body is very significant leading to much greater damage than the direct damage by the incident ions. The secondary electron yield is found to be proportional to the rate of energy loss of the incident particles [3]. This energy loss is connected to the excitation and ionization processes of the target atoms and projectile ions, where inner shell ionization is most vital.

Inner shell ionization of target atoms are being carried out for a long time with light as well as heavy projectiles, for examples [4–14]. It has enabled the research community to study the processes like ionization, excitation, multiple ionization [15], radiative decay, Auger-decay [16], changes in atomic parameters, intrashell coupling effect (in L- and M-shell not in K-shell) [17, 18], etc at different energy regimes. In the present work, we have measured the K-shell x-ray yields of target atoms in three projectile-target systems, i.e., Si + Cu, Si + Zn, and Si + Ge. Using K x-ray yields, we have determined the K-shell ionization cross-section of the target atoms. It is observed that the present measurements are about a factor of three higher than the theoretical direct ionization cross-sections. Such a large discrepancy is a matter of concern to date and needs to be resolved not only for

fundamental understanding, but also for practical implications in heavy-ion induced x-ray emission techniques for elemental analysis.

## II. EXPERIMENTAL DETAILS

The experiment was performed in the atomic physics beam line of 15 UD Pelletron which is situated at Inter-University Accelerator Centre, New Delhi (India). Si ion beam of charge state  $8^+$  for beam energies 84, 90, 98, 107 MeV and charge state  $12^+$  for beam energies 118, 128, 140 MeV was obtained from Pelletron to bombard the natural Cu, Zn, and Ge targets. The vacuum of the order of  $10^{-6}$  Torr was maintained in the chamber using a turbo-molecular pump. Two silicon surface barrier detectors were placed at  $\pm 7.5^\circ$  with respect to beam direction to normalize the charge. A Si(Li) solid state detector was placed outside the chamber at  $125^\circ$  with respect to beam direction and distance of 170 mm from the target. A collimator of 5 mm diameter was placed in front of the detector inside the chamber. The thickness of the Mylar window of the chamber for the detector was 6  $\mu\text{m}$ . The specification of the detector (ORTEC, Oak Ridge, Tennessee, USA) is as follows: thickness 5 mm, diameter 10 mm, the thickness of Be window 25  $\mu\text{m}$  and energy resolution 200 eV for Mn  $K_\alpha$  x-rays. The energy calibration of the detector was done before and after the experiment using the  $^{55}\text{Fe}$ ,  $^{57}\text{Co}$  and  $^{241}\text{Am}$  radioactive sources. The target surface was placed at  $90^\circ$  to the beam direction (normal to the target surface is collinear to the beam direction) on a rectangular steel ladder which could move horizontal and vertical direction with the help of a stepper motor. The spectroscopically pure (99.999%) thin targets of natural Cu, Zn, and Ge were made on the carbon backing using vacuum deposition technique. The thickness of Cu, Zn, Ge, and carbon backing was 25  $\mu\text{g}/\text{cm}^2$ , 14.4  $\mu\text{g}/\text{cm}^2$ , 99  $\mu\text{g}/\text{cm}^2$ , and 20  $\mu\text{g}/\text{cm}^2$ , respectively. The thicknesses of targets were measured using the energy loss method using  $^{241}\text{Am}$  radioactive source. The data was acquired using a PC based software developed at IUAC [19]. The beam current was

\* Email: nanditapan@gmail.com. Present address: 1003 Regal, Mapsko Royal Ville, Sector-82, Gurgaon-122004, India.

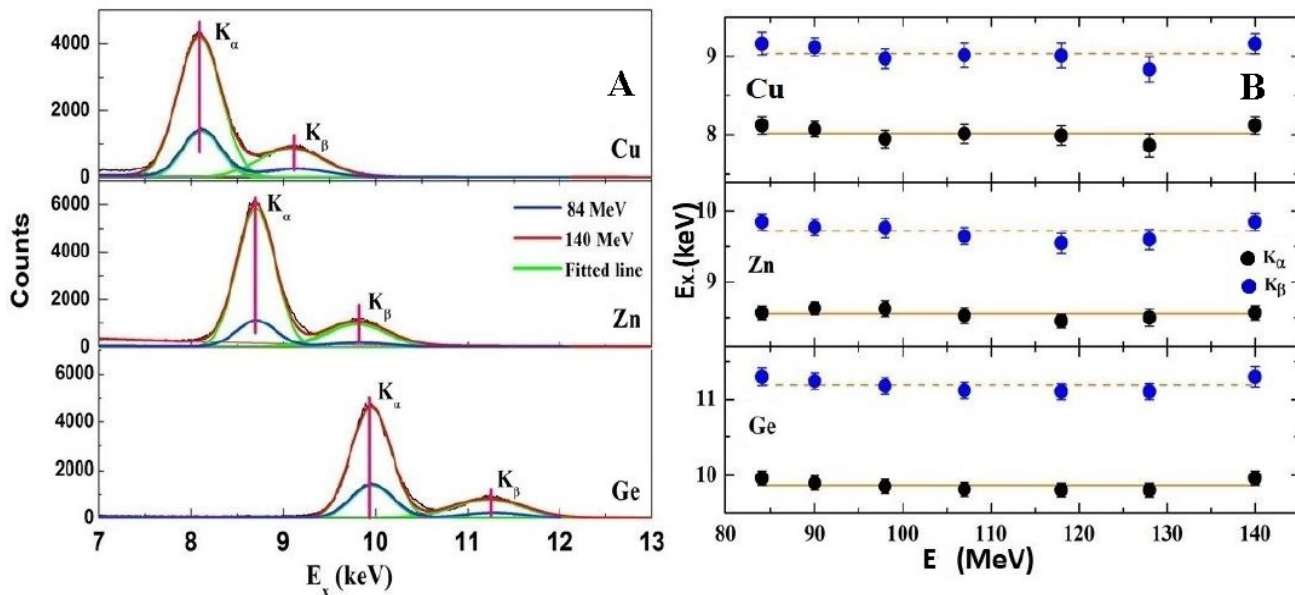


FIG. 1: (A) Typical K x-ray spectra of natural Cu, Zn, and Ge targets when bombarded with 84 and 140 MeV  $^{28}\text{Si}$  ions; (B) x-ray peak energy shift in these targets as a function of the ion-beam energies of  $^{28}\text{Si}$  ions. The solid and dotted orange lines in the right panel show the mean value of the  $K_\alpha$  and  $K_\beta$  peak energies.

kept below 1 nA to avoid pile-up effects and damage to the targets. A semi-empirical fitted relative efficiency curve used for the present measurement can be seen in Oswal *et al.* [13].

### III. DATA ANALYSIS, RESULT, AND DISCUSSION

Typical K x-ray spectra of Cu, Zn, and Ge bombarded with 84 MeV and 140 MeV Si ions are shown in Fig.1. The spectra were analyzed with a nonlinear least-squares fitting method considering a Gaussian line shape for the x-ray peaks and a linear background fitting. The x-ray production cross-sections for the K x-ray lines were determined from the relation,

$$\sigma_i^x = \frac{Y_i^x A}{N_A \epsilon n_p t \beta} \quad (1)$$

here  $Y_i^x$  is the intensity of  $i^{\text{th}}$  x-ray peak ( $i = K_\alpha, K_\beta$ ).  $A$  is the atomic weight of the target.  $N_A$  and  $n_p$  denote the Avogadro number and the number of incident projectiles, respectively.  $\epsilon$ ,  $t$ , and  $\beta$  represent the effective efficiency of the x-ray detector, the target thickness in  $\mu\text{g}/\text{cm}^2$ , and the correction factor for energy-loss of the incident projectile and absorption of emitted x-rays in the target element, respectively. The sum of  $\sigma_{K_\alpha}^x$  and  $\sigma_{K_\beta}^x$  gives a measure of the total K x-ray production cross-section as given in Table I.

It is now well known that heavy ions produce simultaneous multiple ionization (SMI) in several shells while travelling through the target. SMI of L-shells along with

a vacancy in K-shell will influence the value of K-shell fluorescence yield ( $\omega_K$ ) to a considerable extent. Instead of using rigorous Hartree-Fock-Slater calculation for the  $K_\alpha$  and  $K_\beta$  peak shift due to the SMI effect, we employ a simple model of Burch *et al.* [20]. According to it, the energy shift of  $K_\alpha$  and  $K_\beta$  lines per  $2p$  vacancy with respect to corresponding diagram lines are  $1.66Z_L$  and  $4.18Z_L$  eV, respectively, where  $Z_L = Z_2 - 4.15$ ;  $Z_2$  is the atomic number of the target element. It is clear from Fig.1(A) that  $K_\alpha$  and  $K_\beta$  lines are well resolved for all the targets used in the present measurements.

In order to visualize the centroid shift due to the SMI effect, we have plotted the  $K_\alpha$  and  $K_\beta$  energies versus beam energy for all the targets in Fig.1(B). These data are also given in Table II. We notice, for all the targets, the corresponding centroid energies do not vary much with the beam energies used. The average  $K_\alpha$  peak energies of Cu, Zn, and Ge are  $8.01 \pm 0.1$ ,  $8.55 \pm 0.1$ , and  $9.87 \pm 0.1$  keV, respectively and are close to the corresponding diagram  $K_\alpha$  lines at 8.03, 8.62, 9.86 keV. In contrast, this picture for  $K_\beta$  lines is rather distinctive. The mean of the measured  $K_\beta$  lines  $9.04 \pm 0.13$ ,  $9.72 \pm 0.12$ , and  $11.2 \pm 0.1$  keV for Cu, Zn and Ge, respectively are higher than the corresponding diagram  $K_\beta$  lines at 8.905, 9.572, and 10.982 keV. Thus, the difference between the measured  $K_\beta$  and the diagram  $K_\beta$  lines for Cu, Zn, and Ge are 135, 148, and 218 eV, respectively. These values are somewhat larger than the energy shift per  $2p$  vacancy for  $K_\beta$  lines, which are 104, 108, 116 eV, respectively, for Cu, Zn, and Ge.

Energy shifts along with the measurement uncertainty mentioned above imply that on average two vacancies oc-

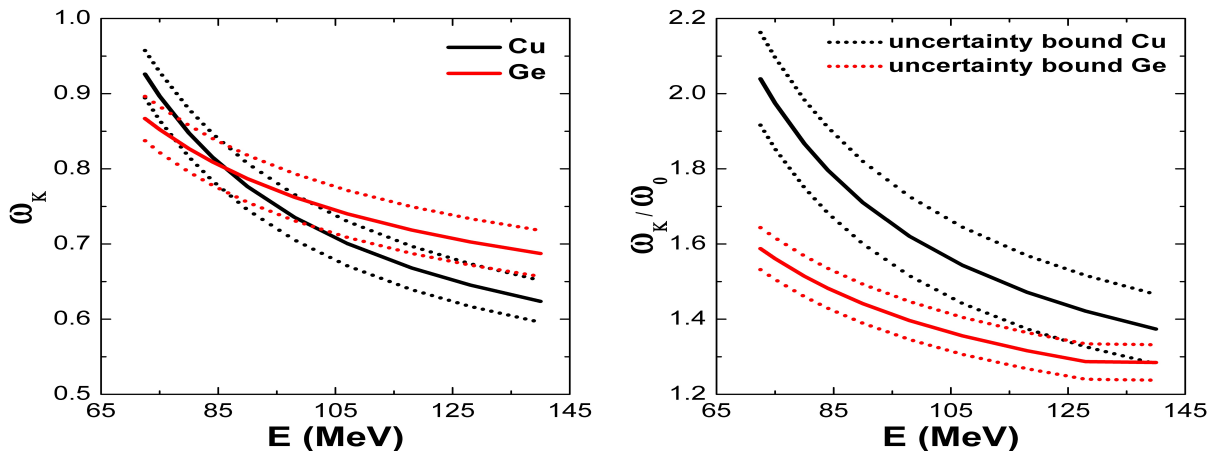


FIG. 2: Variation of  $\omega_K$  and ratio of  $\omega_K$  to  $\omega_0$  with respect to projectile energy (E)

cur in  $2p$  shells during the present collisions. This picture corroborates well the scenario in the  $K_\alpha$  case too as the energy shift per  $2p$  vacancy in Cu, Zn and Ge for  $K_\alpha$  line are only 41, 43, 46 eV, respectively, and the energy shift due to two  $2p$  vacancies will be smeared in its measurement uncertainty of about 100 eV. Thus the SMI must be included in data analysis.

Theoretically, K x-ray production cross-section ( $\sigma_K^x$ ) can be obtained using the relation [6]

$$\sigma_K^x = \omega_K \sigma_K^I \quad (2)$$

here  $\sigma_K^I$  is K-shell ionization cross-section,  $\omega_K$  is the K shell fluorescence yield in the presence of SMI effect in L-shell. Single vacancy fluorescence yield  $\omega_K^0$  given by Krause [22] has been used. Hence, to extract the K shell ionization cross-section from the measured x-ray production cross-section one needs the accurate knowledge of  $\omega_K$ .

To estimate  $\omega_K$  amidst the SMI process discussed above, we follow the description of Lapicki *et.al.* [15] using an assumption that each electron in a manifold of outer subshells is ionized with an identical probability  $P$  and correct  $\omega_K$  in presence of SMI process becomes

$$\omega_K = \frac{\omega_K^0}{1 - P(1 - \omega_K^0)}. \quad (3)$$

With

$$P = q_m^2 \left(1 - \frac{0.225}{v_1^2}\right) \times \frac{1}{1.8v_1^2} \quad (4)$$

here  $v_1 = 6.351[E/A_1]^{1/2}$  (E and  $A_1$  are projectile energy and mass in MeV and amu units, respectively) is the projectile velocity.  $q_m$  is the mean charge state of the projectile ion inside the target.

The uncertainty in  $\omega_K$  can be estimated from the fol-

lowing expression

$$\frac{\Delta\omega_K}{\omega_K} = \frac{\Delta\omega_K^0}{\omega_K^0} + \frac{P}{[1 - P(1 - \omega_K^0)]} \times \left[\frac{\Delta P}{P} \times (1 - \omega_K^0) - \frac{\Delta\omega_K^0}{\omega_K^0}\right] \quad (5)$$

where

$$\frac{\Delta P}{P} = \frac{2\Delta q_1}{q_1}. \quad (6)$$

and the uncertainty in  $\frac{\omega_K}{\omega_K^0}$  can be obtained as follows

$$\frac{\Delta(\omega_K/\omega_K^0)}{\omega_K/\omega_K^0} = \frac{\Delta\omega_K}{\omega_K} [1 - \{\frac{\omega_K^0}{\omega_K}\}^2] \quad (7)$$

The projectile velocity  $v_1$  can be defined very precisely and thus its uncertainty is nominal ( $< 1\%$ ) and taken as just a constant here. For Cu,  $\frac{\Delta\omega_K^0}{\omega_K^0}$  is  $\approx 5\%$  and this is  $\approx 3\%$  for Zn and Ge. If we assume  $\frac{\Delta q_1}{q_1}$  is  $\approx 3\%$  (its estimation and probable uncertainty will be discussed later),  $\frac{\Delta\omega_K}{\omega_K}$  turns out to be  $\approx 6\%$ . Fig. 2 shows the variation of  $\omega_K$  and  $\frac{\omega_K}{\omega_K^0}$  as a function of projectile energy (E). The uncertainty bound is also shown in the figure also.

The inner-shell vacancies are produced predominantly by the direct Coulomb ionization process, which can be treated perturbatively using the first-order perturbation approaches, namely, the plane-wave Born approximation (PWBA) [24]. The standard PWBA approach for direct ionization was further developed to include the hyperbolic trajectory of the projectile, the relativistic wave functions, and the corrections for the binding-polarization effect. The most advanced approach based on the PWBA, which goes beyond the first-order treatment to include the corrections for the binding-polarization effects within the perturbed stationary states (PSS) approximation, the projectile energy loss

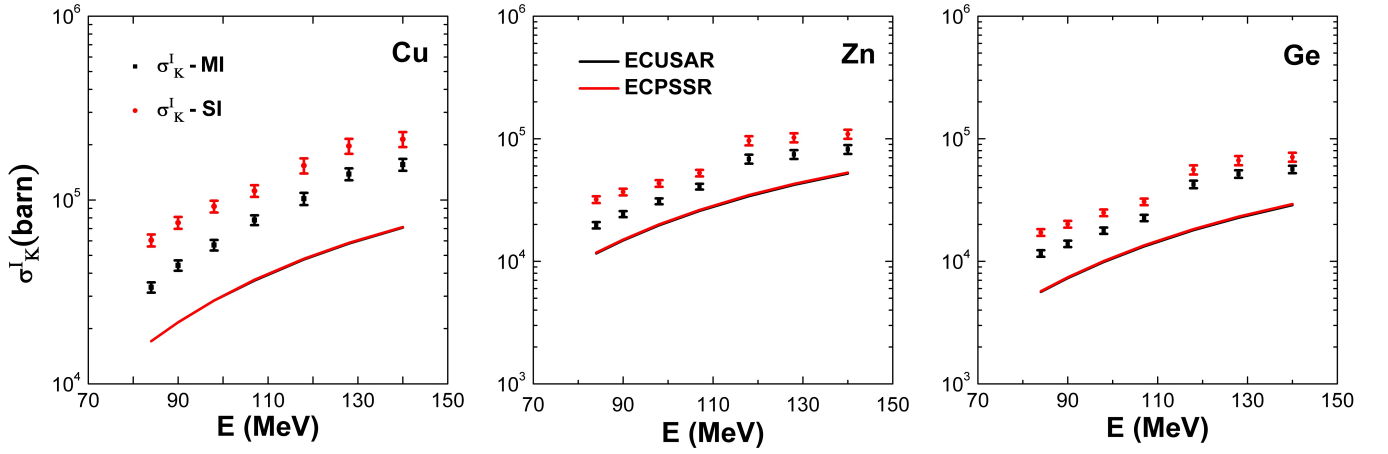


FIG. 3: Comparison of experimental K shell ionization cross-sections ( $\sigma_K$ ) of different targets bombarded by the  $^{28}\text{Si}$  ions as a function of ion-beam energies with the direct ionization cross-sections from ECUSAR [15] and ECPSSR [21]. Here  $\sigma_{K\text{-SI}}$  and  $\sigma_{K\text{-MI}}$  indicate K shell ionization cross-sections with a single K-vacancy and with a single K-vacancy along with several vacancies in higher shells, respectively.

TABLE I: Measured K shell production cross-sections ( $\sigma_K^x$ ) for Cu, Zn, and Ge targets with corresponding multiple ionization probabilities, modified fluorescence yields for multiple ionization [15] and ionization cross-sections ( $\sigma_K^I$ ) by  $^{28}\text{Si}$  ions at different energies ( $E$ ) (MeV). Single vacancy fluorescence yields ( $\omega_K^0$ ) for Cu, Zn, and Ge are 0.454, 0.486, and 0.546, respectively [22], which very closed to Cipolla [23] values 0.44, 0.474, and 0.535, respectively. The cross-sections are in units of Kilobarn/atom.

Cu										
E	$\sigma_K^x$	$\omega_K^0$	$\sigma_K^I - SI$	P	$\omega_K$	$\sigma_K^I - MI$	ECUSAR	$\frac{ECUSAR}{\sigma_K^I - SI}$	$\frac{ECUSAR}{\sigma_K^I - MI}$	
84	27.4±1.4	0.454	60.4±4.5	0.817	0.816±0.03	33.5±2.2	17.1	0.283	0.510	
90	34.2±1.8	0.454	75.3±5.6	0.776	0.780±0.03	44.07±2.9	21.6	0.287	0.491	
98	41.9±2.2	0.454	92.3±6.8	0.736	0.738±0.03	56.89±3.8	28.4	0.308	0.500	
107	50.5±2.6	0.454	112.2±8.2	0.649	0.701±0.03	77.8±4.8	36.5	0.325	0.469	
118	69.9±5.3	0.454	153.9±14.5	0.590	0.668±0.03	101.6±7.7	47.5	0.301	0.468	
128	89.3±6.8	0.454	196.7±18.5	0.547	0.645±0.03	138.4±10.2	58.0	0.295	0.419	
140	97.2±7.3	0.454	214.1±20.0	0.501	0.624±0.03	155.8±11.6	70.9	0.331	0.455	
Zn										
84	15.5±0.8	0.486	31.9±2.0	0.785	0.811±0.02	19.7±1.2	11.6	0.364	0.590	
90	17.9±0.9	0.486	36.8±2.3	0.736	0.779±0.02	24.3±1.4	14.8	0.403	0.610	
98	21.0±1.1	0.486	43.2±2.7	0.680	0.745±0.02	30.9±1.7	19.7	0.456	0.637	
107	25.5±1.3	0.486	52.5±3.3	0.626	0.715±0.02	40.7±2.2	25.8	0.492	0.634	
118	46.9±3.7	0.486	96.5±8.3	0.571	0.686±0.02	68.4±5.7	34.0	0.353	0.498	
128	49.6±3.9	0.486	102.1±8.7	0.529	0.666±0.02	74.5±6.2	42.1	0.412	0.565	
140	53.0±4.1	0.486	109.1±9.3	0.486	0.647±0.02	81.9±6.8	52.0	0.477	0.635	
Ge										
84	9.4±0.5	0.546	17.2±1.0	0.724	0.809±0.02	11.6±710	5.6	0.328	0.486	
90	11.0±0.6	0.546	20.1±1.2	0.679	0.787±0.02	13.9±0.8	7.3	0.363	0.525	
98	13.6±0.7	0.546	24.9±1.5	0.632	0.762±0.02	17.8±0.1	9.9	0.397	0.556	
107	16.7±0.9	0.546	30.6±1.9	0.581	0.740±0.02	22.6±0.1	13.3	0.434	0.587	
118	30.5±0.2	0.546	55.9±4.8	0.534	0.717±0.02	42.5±0.3	18.0	0.322	0.423	
128	36.3±2.8	0.546	66.5±5.7	0.495	0.703±0.02	51.6±3.6	22.7	0.341	0.440	
140	38.7±3.0	0.546	70.9±6.0	0.456	0.687±0.02	56.3±4.0	28.8	0.406	0.511	

(E), and Coulomb deflection (C) effects as well as the relativistic (R) description of inner-shell electrons, is known as the ECPSSR theory [21]. This theory is further modified to replace the PSS effect by a united and separated atom (USA) treatment (ECUSAR) and valid in the com-

plementary collision regimes of slow and intermediate to fast collisions, respectively [15].

In Fig. 3, the measured  $\sigma_K^I$  are plotted as a function of the beam energies, where the overall experimental uncertainty in the present cross-section measurements

TABLE II: Energy  $E_x$  (keV) of  $K_\alpha$  and  $K_\beta$  x-rays of Cu, Zn and Ge targets for different beam energies (E) in MeV of  $^{28}\text{Si}$  projectile. Their mean error of average energy of Cu, Zn, Ge for  $K_\alpha$  and  $K_\beta$  in keV are  $(8.01 \pm 0.1, 9.04 \pm 0.13)$ ,  $(8.55 \pm 0.1, 9.72 \pm 0.12)$  and  $(9.87 \pm 0.1, 11.2 \pm 0.1)$ , respectively.  $K_\alpha$  and  $K_\beta$  energy of Cu, Zn and Ge targets in keV are (8.048, 8.905), (8.639, 9.572), and (9.886, 10.982), respectively.

E	Cu		Zn		Ge	
	$K_\alpha$	$K_\beta$	$K_\alpha$	$K_\beta$	$K_\alpha$	$K_\beta$
84	$8.12 \pm 0.11$	$9.12 \pm 0.14$	$8.57 \pm 0.1$	$9.85 \pm 0.11$	$9.96 \pm 0.10$	$11.31 \pm 0.12$
90	$8.07 \pm 0.10$	$9.12 \pm 0.12$	$8.63 \pm 0.09$	$9.77 \pm 0.11$	$9.90 \pm 0.10$	$11.25 \pm 0.11$
98	$7.94 \pm 0.11$	$8.98 \pm 0.12$	$8.62 \pm 0.11$	$9.76 \pm 0.13$	$9.85 \pm 0.10$	$11.18 \pm 0.11$
107	$8.01 \pm 0.12$	$9.02 \pm 0.15$	$8.52 \pm 0.11$	$9.65 \pm 0.12$	$9.81 \pm 0.10$	$11.12 \pm 0.11$
118	$7.99 \pm 0.12$	$9.01 \pm 0.15$	$8.45 \pm 0.09$	$9.55 \pm 0.14$	$9.80 \pm 0.10$	$11.11 \pm 0.11$
128	$7.86 \pm 0.15$	$8.8 \pm 0.16$	$8.50 \pm 0.12$	$9.60 \pm 0.14$	$9.80 \pm 0.10$	$11.11 \pm 0.11$
140	$8.12 \pm 0.11$	$9.2 \pm 0.13$	$8.57 \pm 0.1$	$9.85 \pm 0.13$	$9.96 \pm 0.10$	$11.31 \pm 0.13$

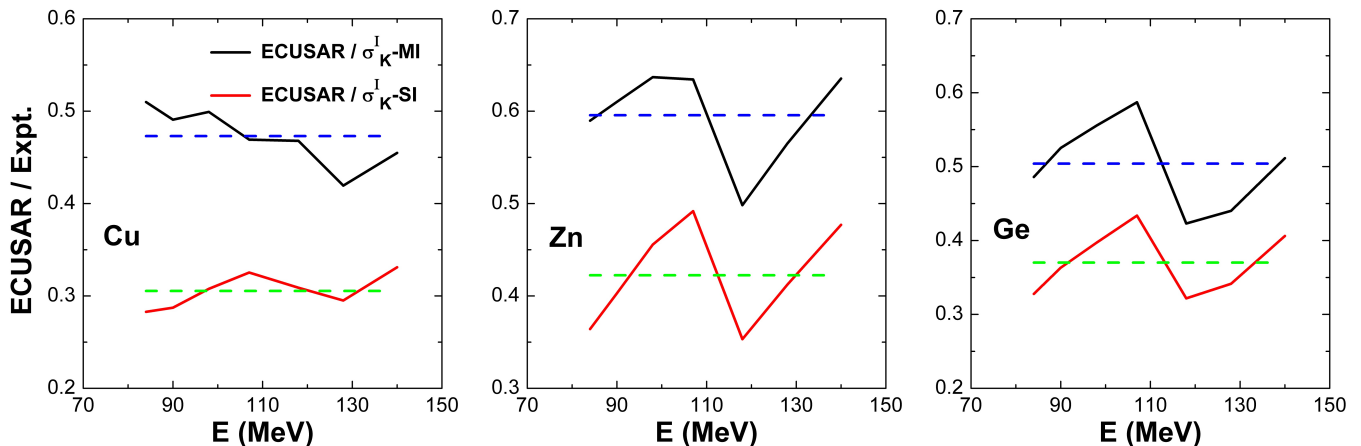


FIG. 4: Ratio of theoretical (ECUSAR) ionization cross-sections to the experimental ionization cross-sections is plotted as a function of beam energy. Experimental ionization cross sections are evaluated for single ionization in K-shell as well as for single ionization in K-shell plus certain ionization in higher shells. Green and blue dashed lines indicate the average line for the ratio of theoretical ionization cross-sections to the experimental ionization cross-sections for single and multiple ionization, respectively.

is attributed to the uncertainties in the photopeak, absolute efficiency of the detector, charge collected in Faraday cup, and target thickness. We have compared the measured  $\sigma_K^I$  with the predictions of direct ionization cross-section from the theories ECPSSR and ECUSAR using the ISICS00 code [25]. We can see that the ECPSSR and ECUSAR predictions are almost equal. It just proves the fact that though  $Z_1/Z_2$  for the systems used in the present experiment be in favour of united atom situation but at 3-5 MeV/u energy it ought to behave as the separated atom and thus the ECUSAR values are almost the same as the ECPSSR figures. Fig. 4 shows the ratio of theoretical (ECUSAR) ionization cross-sections to the experimental ionization cross-sections considering the fluorescence yield with single vacancy only in K-shell as well as with single vacancy in K-shell along with other vacancies in higher shells. In former case on the average the ratio is equal to 0.31, 0.42 and 0.37, respectively for Cu, Zn and Ge. Whereas the ratios are increased to 0.48, 0.60 and 0.51, respectively for Cu, Zn and Ge.

As mentioned above, the measured  $\sigma_K^I$  are much higher than the predictions. Further, we found that such findings are not at all observed for the first time. In recent years a series of measurements by the Kazakhstan group [26–28] showed this fact very clearly in argon, Krypton and Xenon induced x-ray production cross-section measurements. The scenario becomes clearer when one reads the changes from light proton induced ionization [29] to heavy xenon induced cases [28] through nitrogen [30], oxygen [31], neon [32], argon [26] and krypton [27]. More importantly, the difference between the experiment and prediction is not only in the case of K-shell x-ray production cross sections but also in L-shell and M-shell x-ray production cross sections too. Gornachev *et al.* [28] attributed the difference observed in the case of symmetric partners to the molecular mechanisms of the ion-atom interaction when mutual distortion of the atomic orbitals of the colliding partners can take place and the formation of a quasi molecule is expected. For the asymmetric and slow collisions, where  $Z_1 \gg Z_2$  and  $v_1/v_{2S} \leq 1$ , the effect

of electron capture of the target electrons to the vacant projectile shells becomes important. Further, accounting the multiple ionization of the target atoms by heavy ions is also important. All these effects may lead to a big change in the x-ray productions. Recently, Masekane *et al.* [33] has attempted to take electron capture into account for the K-shell ionization. We have addressed this issue in a forthcoming article in a greater detail [34].

#### IV. CONCLUSION

We have measured K-shell ionization by heavy-ion impact. Here, the targets Cu, Zn, and Ge were bombarded by the 84-140 MeV  $^{28}\text{Si}$  ions to measure K-shell production cross-sections. We observed that the measured ionization cross-sections differ by at least a factor of two and

three times higher than the theoretical direct ionization cross-sections if multiple ionization effects are taken and not taken into account. Electron capture from the target K-shell to the K- and L-shell of the projectile ions may be required to consider in resolving this difference. Appropriate theoretical work is extremely welcome to address this issue not only for fundamental understanding but also for practical applications in heavy-ion induced x-ray emission techniques for elemental analysis.

#### V. ACKNOWLEDGEMENTS

We acknowledge cooperation from the Pelletron accelerator staff during the experiments. S.S. gratefully acknowledges one of his supervisors B. R. Behera for his support throughout this work.

- 
- [1] J. Miranda, O. De Lucio, and M. Lugo-Licona, *Revista mexicana de física* **53**, 29 (2007).
- [2] G. Kraft, *Progress in particle and Nuclear Physics* **45**, S473 (2000).
- [3] E. Sternglass, *Physical Review* **108**, 1 (1957).
- [4] O. Benka and A. Kropf, *Atomic Data and Nuclear Data Tables* **22**, 219 (1978).
- [5] I. Orlic, C. Sow, and S. Tang, *Atomic data and nuclear data tables* **56**, 159 (1994).
- [6] U. Kadhane, C. Montanari, and L. C. Tribedi, *Physical Review A* **67**, 032703 (2003).
- [7] G. Lapicki, *X-Ray Spectrometry: An International Journal* **34**, 269 (2005).
- [8] X. Zhou, Y. Zhao, R. Cheng, Y. Wang, Y. Lei, X. Wang, and Y. Sun, *Nuclear Instruments and Methods in Physics Research Section B: Beam Interactions with Materials and Atoms* **299**, 61 (2013).
- [9] M. Msimanga, C. Pineda-Vargas, and M. Madhuku, *Nuclear Instruments and Methods in Physics Research Section B: Beam Interactions with Materials and Atoms* **380**, 90 (2016).
- [10] S. Kumar, U. Singh, M. Oswal, G. Singh, N. Singh, D. Mehta, T. Nandi, and G. Lapicki, *Nuclear Instruments and Methods in Physics Research Section B: Beam Interactions with Materials and Atoms* **395**, 39 (2017).
- [11] M. Oswal, S. Kumar, U. Singh, G. Singh, K. Singh, D. Mehta, D. Mitnik, C. C. Montanari, and T. Nandi, *Nuclear Instruments and Methods in Physics Research Section B: Beam Interactions with Materials and Atoms* **416**, 110 (2018).
- [12] M. Hazim, C. Koumeir, A. Guertin, V. Métivier, A. Naja, N. Servagent, and F. Haddad, *Nuclear Instruments and Methods in Physics Research Section B: Beam Interactions with Materials and Atoms* **479**, 120 (2020).
- [13] M. Oswal, S. Kumar, U. Singh, S. Singh, G. Singh, K. Singh, D. Mehta, A. Mendez, D. Mitnik, C. Montanari, *et al.*, *Radiation Physics and Chemistry* **176**, 108809 (2020).
- [14] J. Miranda, D. Serrano, J. Pineda, D. Marín-Lámbarri, L. Acosta, J. Mendoza-Flores, S. Reynoso-Cruces, and E. Chávez, *Nuclear Instruments and Methods in Physics Research Section B: Beam Interactions with Materials and Atoms* **477**, 23 (2020).
- [15] G. Lapicki, G. R. Murty, G. N. Raju, B. S. Reddy, S. B. Reddy, and V. Vijayan, *Physical Review A* **70**, 062718 (2004).
- [16] P. Dahl, M. Rodbro, G. Hermann, B. Fastrup, and M. Rudd, *Journal of Physics B: Atomic and Molecular Physics* **9**, 1581 (1976).
- [17] M. Pajek, D. Banaś, J. Semaniak, J. Braziewicz, U. Majewska, S. Chojnacki, T. Czyżewski, I. Fijał, M. Jaskóła, A. Glombik, *et al.*, *Physical Review A* **68**, 022705 (2003).
- [18] L. Sarkadi and T. Mukoyama, *Journal of Physics B: Atomic and Molecular Physics* **14**, L255 (1981).
- [19] E. Subramaniam and B. Kumar, *Nucl. Phys* **117** (2010).
- [20] D. Burch, L. Wilets, and W. Meyerhof, *Physical Review A* **9**, 1007 (1974).
- [21] W. Brandt and G. Lapicki, *Physical Review A* **23**, 1717 (1981).
- [22] M. O. Krause, *Journal of physical and chemical reference data* **8**, 307 (1979).
- [23] S. J. Cipolla, *Computer Physics Communications* **182**, 2439 (2011).
- [24] B.-H. Choi, E. Merzbacher, and G. Khandelwal, *Atomic Data and Nuclear Data Tables* **5**, 291 (1973).
- [25] M. Batič, M. G. Pia, and S. J. Cipolla, *Computer Physics Communications* **183**, 398 (2012).
- [26] N. Gluchshenko, I. Gorchachev, I. Ivanov, A. Kireyev, S. Kozin, A. Kurakhmedov, A. Platov, and M. Zdorovets, *Nuclear Instruments and Methods in Physics Research Section B: Beam Interactions with Materials and Atoms* **372**, 1 (2016).
- [27] I. Gorchachev, N. Gluchshenko, I. Ivanov, A. Kireyev, V. Alexandrenko, A. Kurakhmedov, A. Platov, and M. Zdorovets, *Nuclear Instruments and Methods in Physics Research Section B: Beam Interactions with Materials and Atoms* **407**, 86 (2017).

- [28] I. Gorlachev, V. Alexandrenko, N. Gluchshenko, I. Ivanov, A. Kireyev, M. Krasnopyorova, A. Kurakhmedov, A. Platov, and M. Zdorovets, *Nuclear Instruments and Methods in Physics Research Section B: Beam Interactions with Materials and Atoms* **430**, 31 (2018).
- [29] E. Batyrbekov, I. Gorlachev, I. Ivanov, and A. Platov, *Nuclear Instruments and Methods in Physics Research Section B: Beam Interactions with Materials and Atoms* **325**, 84 (2014).
- [30] E. Batyrbekov, N. Gluchshenko, I. Gorlachev, I. Ivanov, and A. Platov, *Nuclear Instruments and Methods in Physics Research Section B: Beam Interactions with Materials and Atoms* **330**, 86 (2014).
- [31] I. Gorlachev, N. Gluchshenko, I. Ivanov, A. Kireyev, S. Kozin, A. Kurakhmedov, A. Platov, and M. Zdorovets, *Nuclear Instruments and Methods in Physics Research Section B: Beam Interactions with Materials and Atoms* **381**, 34 (2016).
- [32] I. Gorlachev, N. Gluchshenko, I. Ivanov, A. Kireyev, M. Krasnopyorova, A. Kurakhmedov, A. Platov, Y. Sambayev, and M. Zdorovets, *Nuclear Instruments and Methods in Physics Research Section B: Beam Interactions with Materials and Atoms* **448**, 19 (2019).
- [33] M. Masekane, S. Moloi, M. Madhuku, and M. Msimanga, *Radiation Physics and Chemistry* **176**, 109083 (2020).
- [34] S. Chatterjee, S. Singh, P. Sharma, M. Oswal, S. Kumar, M. Claudia, D. Mitra, and T. Nandi, arXiv preprint arXiv:2103.08299 (2021).